International Journal of Advances in Engineering and Management (IJAEM)
Volume 3, Issue 12, pp: 50-57 www.ijaem.net ISSN: 2395-5252

CFD Analysis Of Aircraft Winglet

Saravana Kumar , Imran Naseer , Joshey Heaven , Yasar Arafath , Joemon T Manoj
Department Of Aeronautical Engineering , Hindusthan College Of Engineering And Technology

Date of Submission: 14-11-2021 Date of Acceptance: 29-11-2021

ABSTRACT: The objective of this project is to reduce the lift induced drag generated due to wing tip vortices at the tip of the wing. The NACA-65(3)-218 is chosen as a clean and the analysis of the winglet's flow is calculated at various angles. The unstructured mesh is constructed with the prism layer meshing using ICEM- CFD and the grid independence study has conducted to know the optimum mesh size for the wing configuration of clean wing (NACA-65(3)-218), L-winglets. The RANS (Reynolds average Navier stokes equation) numerical studies have conducted by the finite volume method to analyze the physical system model. Fluent is used as a common solver for analyzing the physical model. The new design changes are implemented with L-winglet attached at the end of the clean wing. The L-winglet is used for the computational analysis. The analysis is carried out at the different cant angles of attack such as 600 ,750 and 900 at an inlet velocity of 150m/s under the adiabatic conditions. The obtained results shows that the 90º L- winglet performs better than the winglets at cant angles of 60º and 75º with the L/D ratio of 8.

I. INTRODUCTION (WINGLETS)

Winglets, it increases the aspect ratio of the wing by maintaining the structural weight within the limits. The lift induced drag can also be reduced by increasing the wing span but it will increase the pressure drag and profile drag on the wings and also increases the weight of the wing. Induced drag takes the major share among the total drag of up-to 40% and therefore it consumes large fuel. Thus by adding the winglet it will increase the aspect ratio of the wing and reduces the lift induced drag. Richard Whitcomb's research in the 1970s at NASA first used winglet with its modern meaning referring to near-vertical extension of the wing tips. The upward angle (or cant) of the winglet, its inward or outward angle (or toe), as well as its size and shape are critical for correct performance and are unique in each application. The wingtip vortex, which rotates around from below the wing, strikes the cambered surface of the winglet, generating a force that angles inward and slightly forward, analogous to a sailboat sailing close hauled. The winglet converts some of the otherwise-wasted energy in the wingtip vortex to an apparent thrust. This small contribution can be worthwhile over the aircraft's lifetime, provided the benefit offsets the cost of installing and maintaining the winglets. Another potential benefit of winglets is that they reduce the intensity of wake vortices. Those trail behind the plane and pose a hazard to other aircraft. Minimum spacing requirements between aircraft operations at airports are largely dictated by these factors. Aircraft are classified by weight (e.g. "Light," "Heavy," etc.) because the vortex strength grows with the aircraft lift coefficient, and thus, the associated turbulence is greatest at low area where the vortex forms upward away from the wing surface, since the center of the resulting vortex is now at the tip of the winglet.

Aircraft such as the Airbus A340 and the Boeing 747-400 use winglets while other designs such as later versions of the Boeing 777 and the Boeing 747-8 have raked wingtips. The fuel economy improvement from winglets increases with the mission length. Blended winglets allow a steeper angle of attack reducing takeoff distance.

FIGURE 1.1

In the earlier days in England Frederick W. Lanchester and others have made lot of studies to reduce the wing tip vortices and suggested that the vertical bodies attached to the wing tip will reduce the induced drag. Hand calculations and the results of experimental studies of the vertical bodies attached at

International Journal of Advances in Engineering and Management (IJAEM)
Volume 3, Issue 12, pp: 50-57 www.ijaem.net ISSN: 2395-5252

the tip of the main wing have proven that it will reduce the induced drag (and Lanchester has patented the concept of endplate in the year 1897). But this was only successful when the aircraft is flying at high speed and in the lower speeds it will increase the profile drag and pressure drag. Thus due to its increase in parasitic drag byadding the endplates it was not much used on later days

II. LITERATURE SURVEY

- Simulations of Various Shapes of Winglets, International Journal of Engineering Research & Technology (IJERT), ISSN: 2278-0181,ETMET - 2016 Conference Proceedings.
- Improving the Aerodynamic Performance of a Wing with Winglet .November 2014International Journal of Natural and Engineering Sciences 8(3):52-57.
- CFD Study of the Impact of Variable Cant Angle Winglets on Total Drag Reduction Joel Guerrero *, Marco Sanguineti and Kevin Wittkowski ; Published: 3 December 2018.
- Bourdin.P,*Gatto.A,*andFriswell.M. I., "Aircraft Control via Variable CantAngle Winglets"Journal of Aircraft,Vol. 45, No. 2, March-April 2008. DOI: 10.2514/1.27720.pp. 414-423.
- Altab Hossain .G, AtaurRahman, A.K.M. Iqbal. P, Ariffin.M, and Mazian.M et.al, "Drag Analysis of an Aircraft Wing Model with and without Bird Feather like Winglet", World Academy of Science, Engineering and Technology International Journal of Mechanical, Industrial Science and Engineering Vol:5 No:9, 2011 .
- Grant.R.H, "Retractable Multiple Winglets",United States Patent Document, Patent No. US2007/0262205, 2007.

III. METHODOLOGY

Here in this work we are focusing to reduce the lift induced drag on the wing i.e., by attaching the L-Winglet at various angles at the tip of the main wing which reduces the vortices generated. In the present work the NACA-65(3)-218 is selected as a base wing and the analysis is carried out for various angles of attack at velocity of 150m/s and the results are estimated.

3.1.Computational Domain & Mesh.

The computational domain for the present study mimics the one used in . Figure 1 shows the 3-D domain.

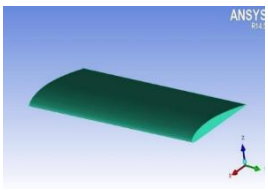

FIGURE 1.2

Dimension	Value
Chord	295 mm
Wing span	794 mm
Wing type	No swept back

TABLE 3.1. EXPERIMENTAL TEST SETUP DETAILS USED

The wind tunnel could be operated at a maximum air speed of 50 m/s and the turntable had a capacity for setting an angle of attack of 140 . The ambient pressure, temperature and humidity were recorded using barometer, thermometer, and hygrometer respectively for the evaluation of air density in the laboratory environment. Details of the experimental results, together with the wing profile used can be seen by the work carried out by Altab Hossain et al

IV. ANSYS® FLUENT 14.5

Firstly, ANSYS® FLUENT 14.5 is used for carrying out simulation & following assumptions are made-(i)the flow is steady, (ii) the fluid is incompressible (iii) the fluid properties are constant. The governing equations used are continuity & momentum, SA is the turbulence model selected as it is best suited for external flow. Coupled algorithm is used for pressure velocity coupling & standard interpolation is used for pressure. Second order upwind scheme is used for, momentum. The convergence criteria fixed is 10-3 for continuity & turbulence quantities, 10-6 for momentum equations. Double precision solver is activated for the simulation.

V. PROCEDURE

Further the NACA-65(3)-218 wing is attached with L-winglets at three different angles to the end of the base wing to carry out the behavioral study of the formation of wing tip vortices which accounts to induced drag. In the first case the NACA-65(3)-218 is attached with the L-winglet of cant angle 600 and the analysis is carried out for various angles of attack 0 0 at the free stream velocity of 150m/s. In the second and third case, the NACA-65(3)-218218 is attached with the L-winglet of cant angle 750 and 900 respectively, and the analysis is carried out under the

International Journal of Advances in Engineering and Management (IJAEM)
Volume 3, Issue 12, pp: 50-57 www.ijaem.net ISSN: 2395-5252

boundary conditions as in the first case. The analysis was focused to study the behavior of formation of wing tip vortices on both the cases which will lead to the formation of the induced drag. Following images show the different cant angles of winglet (60, 70 and 90 degrees).

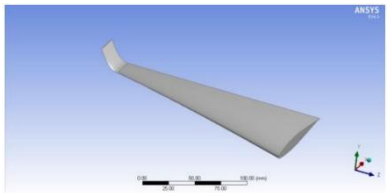

FIGURE5.1 Isolated view of aircraft winglet at cant angle 60º

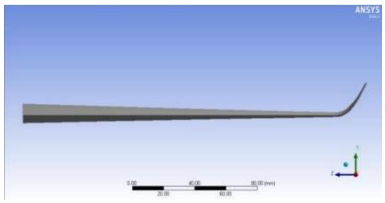

FIGURE5.2 Front view of aircraft winglet at cant angle 60º

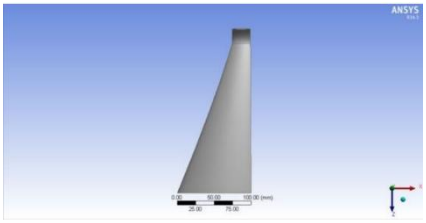

FIGURE5.3 Top view of aircraft winglet at cant angle 60º

The above figure 5.1 shows the isolated view of the winglet at cant angle 60°, where isolated view refers to the solitary view (view from all the angles) of the winglet. Similarly, figure 5.2 shows the front view of the winglet at cant angle 60°, where front view refers to the point of view from the front position of the winglet. The figure 5.3 cited above shows the top view of the winglet at cant angle 60°. All the three views of the winglet are taken for case 1analysis.

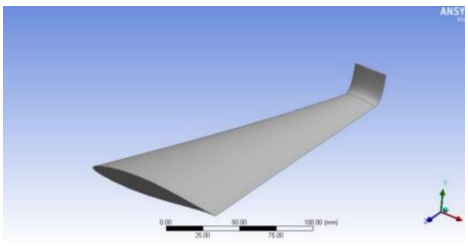

FIGURE5.4 Isolated view of aircraft winglet at cant angle 75º

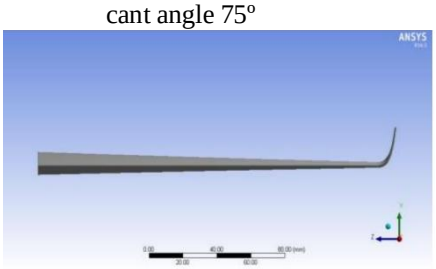

FIGURE5.5 Front view of aircraft winglet at cant angle 75º

FIGURE5.6 Top view of aircraft winglet at cant angle 75 º

The above figure 5.4 shows the isolated view of the winglet at cant angle 75°, where isolated view refers to the solitary view (view from all the angles) of the winglet. The figure 5.5 shows the front view of the winglet at cant angle 75°, where front view refers to the point of view from the front position of the winglet. Similarly, the figure 5.6 cited above shows the top view of the winglet at cant angle 75°. All the three views of the winglet are taken for case 2 analysis.

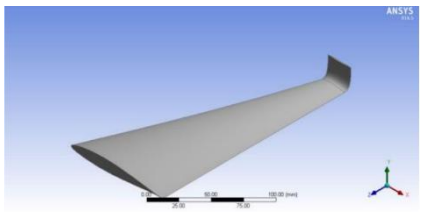

FIGURE5.7 Isolated view of aircraft winglet at cant angle 90º

International Journal of Advances in Engineering and Management (IJAEM)
Volume 3, Issue 12, pp: 50-57 www.ijaem.net ISSN: 2395-5252

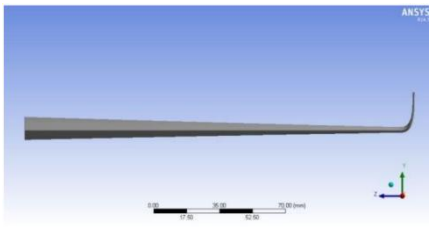

FIGURE5.8 Front view of aircraft winglet at cant angle 90º

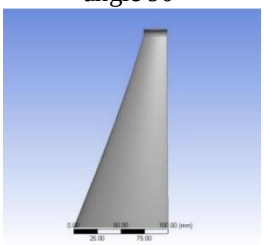

FIGURE5.9 Top view of aircraft winglet at cant angle 90 º

The above figure 5.7 shows the isolated view of the winglet at cant angle 90°, where isolated view refers to the solitary view (view from all the angles) of the winglet. Similarly, figure 5.8 shows the front view of the winglet at cant angle 90°, where front view refers to the point of view from the front position of the winglet. The figure 5.9 cited above shows the top view of the winglet at cant angle 90°. Similar to the above cases, all the three views of the winglet at cant angle 90° are taken for case 3 analysis.

The following images show the boundary conditions of aircraft winglet.

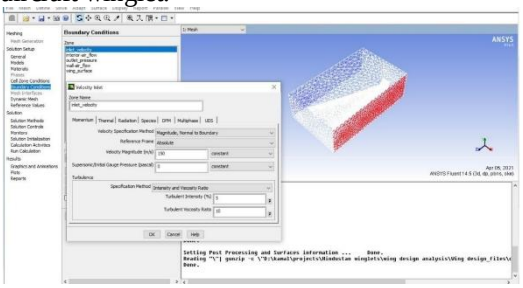

FIGURE5.10 Boundary condition1- inlet velocity

The figure 5.10 cited above shows the boundary condition of the inlet velocity of the winglet. From the figure it is clearly understood that the velocity magnitude is 150 m/s, turbulent intensity is 5% and turbulent viscosity ratio is 10.

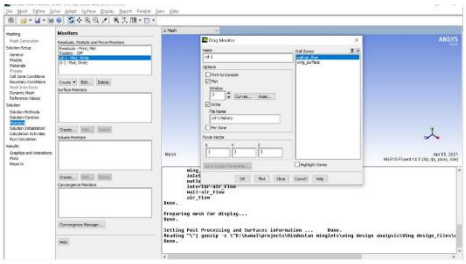

FIGURE5.11 Drag monitor

The figure 5.11 cited above shows the boundary condition of the drag monitor of the winglet. Drag monitor dialog box is used to save the convergence history of the drag co-efficient on specified wall zones. Wall zones contain a selectable list of wall zones on which the selected co- efficient is computed. Here the selected wall zone is wall air flow. Plot specifies whether or not to plot the selected co-efficient in the graphics window after each iteration.

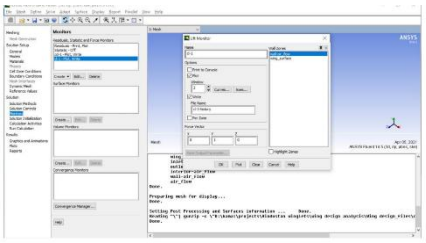

FIGURE5.12 Lift monitor

The figure 5.12 cited above shows the boundary condition of the lift monitor of the winglet. Wall zones contain a selectable list of wall zones on which the selected coefficient is computed. Here the selected wall zone is wall air flow.

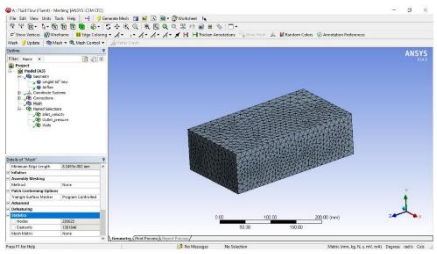

FIGURE5.13 Mesh

The figure 5.13 cited above shows the image of the mesh obtained, where the winglet is to be placed. A mesh is a network that is formed of cells and points. Meshing refers to the process where complex geometries and models are divided into simple elements that can be used as discrete local approximations of the larger domain.

International Journal of Advances in Engineering and Management (IJAEM)
Volume 3, Issue 12, pp: 50-57 www.ijaem.net ISSN: 2395-5252

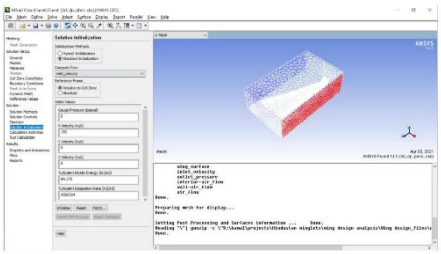

FIGURE5.14 Solution initialization

The figure 5.14 cited above shows the solution initialization of the mesh. The solution initialization task page allows setting initial values for the flow variables and initializing the solution using these values. The user can also indicate whether the specified values for velocities are absolute or relative to the velocity in each cell zone.

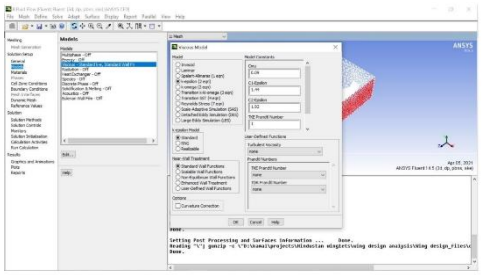

FIGURE5.15 Viscous model

The figure 5.15 cited above shows the viscous model of the mesh. The viscous model allows the user to set parameters of in viscid, laminar and turbulent flow. Model contains options for specifying the viscous model.

VI. RESULTS AND ANALYSIS

This chapter contains the results and analysis of the winglet at different cant angles of 60º,75º and 90º.

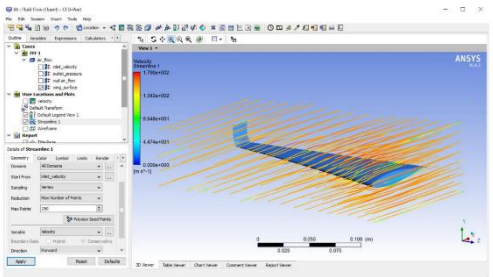

FIGURE6.1 Result screen

The figure 6.1 cited above shows the result screen where the results of the analysis of winglet for each cant angle (60º,75º,90º) will be displayed.

6.1 Analysis of winglet at cant angle 60º

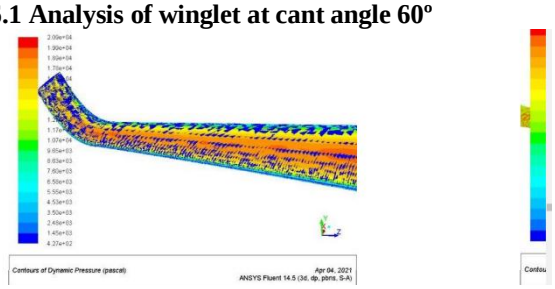

FIGURE6.2 Dynamic pressure

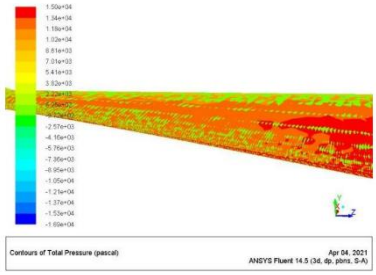

FIGURE6.3 Total pressure

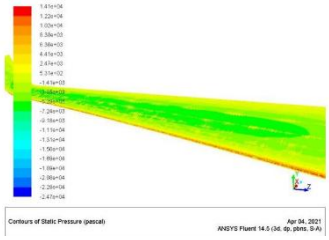

FIGURE 6.4 Static pressure

The above three figures show the different type of pressures that varies on the winglet at cant angle 60°. The figure 6.2 cited above shows the dynamic pressure of the winglet which refers to the excess pressure above ambient that develops when air is compressed and adiabatically brought to rest. The figure 6.4 cited above shows the static pressure of the winglet, where the static pressure, also known as ambient pressure, is always present whether an aircraft is moving or at rest. The figure 6.3 cited above refers to the total pressure of the winglet. Total pressure is the sum of the local atmospheric pressure and the impact pressure caused by the aircraft's motion through the air.

International Journal of Advances in Engineering and Management (IJAEM)
Volume 3, Issue 12, pp: 50-57 www.ijaem.net ISSN: 2395-5252

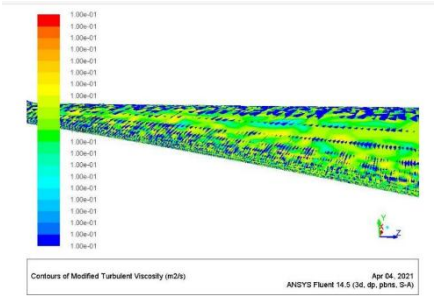

FIGURE 6.5 Turbulence viscosity

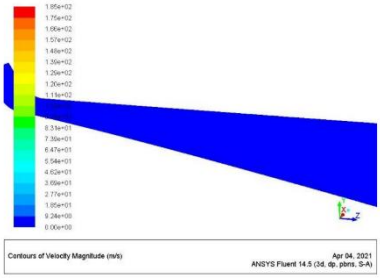

FIGURE 6.6 Contours of Velocity magnitude (m/s)

The figure 6.5 and figure 6.6 cited above refers to the turbulence viscosity and the contours of velocity magnitude of the winglet at cant angle 75° respectively.

6.2 Analysis of winglet at cant angle 75º

The figure 6.7 cited above shows the dynamic pressure of the winglet at cant angle 75°. Dynamic pressure refers to the excess pressure above ambient that develops when air is compressed and adiabatically brought to rest. The figure 6.8 cited above shows the velocity streamline of the winglet at cant angle 75° placed inside the mesh

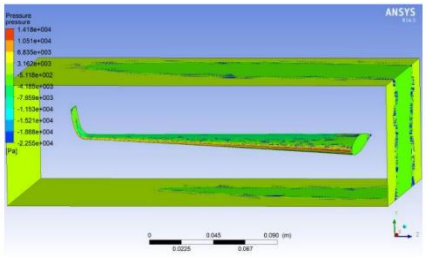

FIGURE 6.7 Dynamic pressure

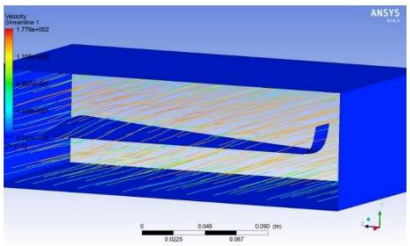

FIGURE 6.8 Velocity streamline

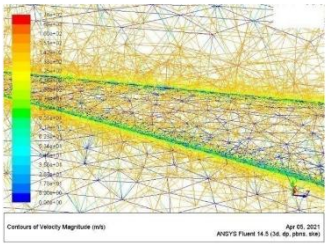

FIGURE 6.9 Velocity(1)

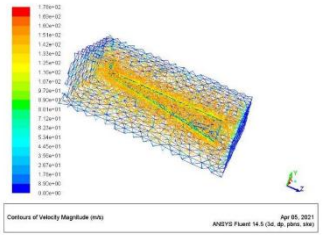

FIGURE 6.10 Velocity(2)

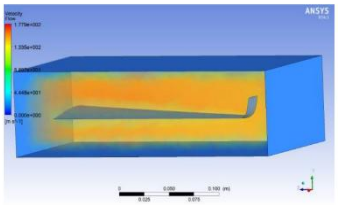

FIGURE 6.11 Velocity(3)

The figure 6.9, the figure 6.10 and the figure 6.11 shows the different velocities of the winglet at cant angle 75° named as velocity 1, velocity 2 and velocity 3 respectively.

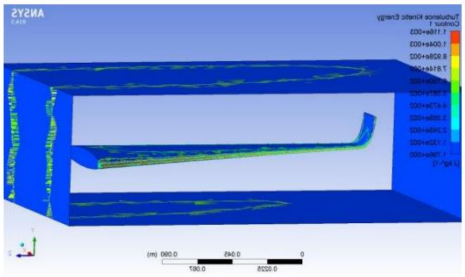

FIGURE 6.12 Turbulence (1)

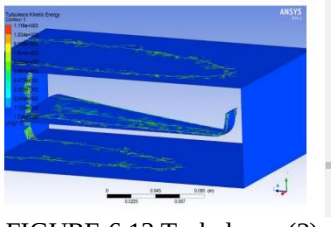

FIGURE 6.13 Turbulence (2)

International Journal of Advances in Engineering and Management (IJAEM)
Volume 3, Issue 12, pp: 50-57 www.ijaem.net ISSN: 2395-5252

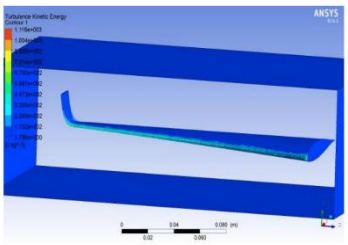

FIGURE 6.14 Turbulence (3)

The figure 6.12, the figure 6.13 and the figure 6.14 shows the different measures of turbulence of the winglet at cant angle 75° named as turbulence 1, turbulence 2 and turbulence 3 respectively. The reduced turbulence from the above figures defines the primary purpose of the winglet to reduce the turbulence at the tip of the vortices.

6.3 Analysis of winglet at cant angle 90º

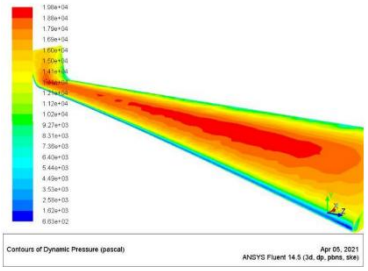

FIGURE 6.15 Dynamic pressure 1

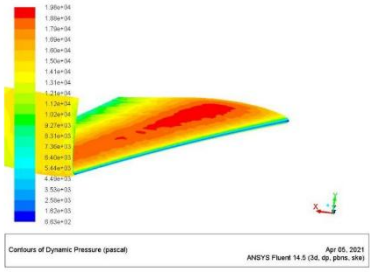

FIGURE 6.16 Dynamic pressure 2

The figure 6.15 and 6.16 cited above shows the dynamic pressures of the winglet at cant angle 90°, where dynamic pressure refers to the excess pressure above ambient that develops when air is compressed and adiabatically brought to rest.

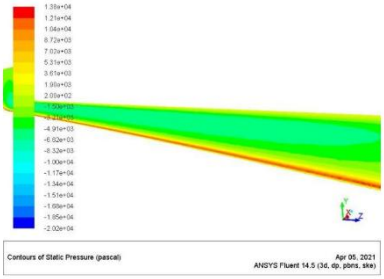

FIGURE 6.17 Static pressure

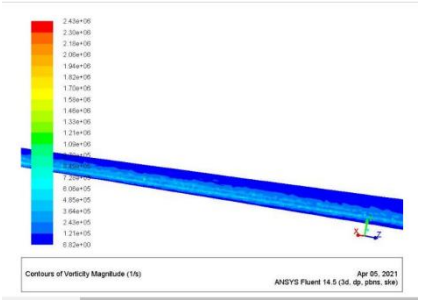

FIGURE 6.18 Viscosity

The figure 6.17 cited above shows the static pressure of the winglet, where the static pressure, also known as ambient pressure, is always present whether an aircraft is moving or at rest. The figure 6.18 shows the viscosity of the winglet at cant angle 90°. In the presence of viscous drag, the winglets produce a small thrust.

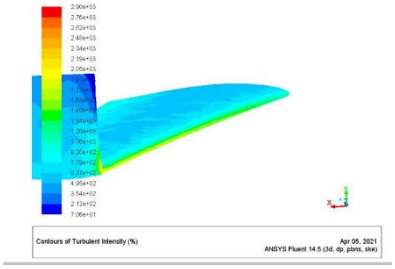

FIGURE 6.19 Turbulent intensity

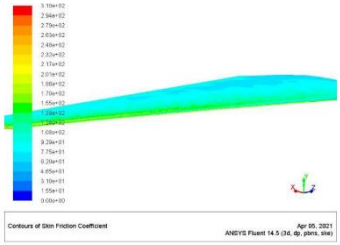

FIGURE 6.20 Skin friction coefficient

The figure 6.19 cited above shows the turbulent intensity of the winglet at cant angle 90°and the figure 6.20 cited above refers to the skin friction co-efficient of the winglet at cant angle 90°.

VII. CONCLUSION

By analyzing the L-winglet at different cant angles such as 60º,75º and 90º, it is concluded that the L- winglet performs better at cant angle of 90º with high L/D ratio of 8 at an angle of attack of 0º. Therefore by adding winglets to the clean wing configuration reduces the lift induced drag produced due to the formation of wing tip vortices by the third direction flow. The results show that by using the concept of variable cant angle, winglet can replace the conventional control surfaces

7.1. FUTURE WORK

This project can be extended in future by analyzing the L/D ratio of winglet at different angles of attack such as 8º,12º,14º and 16º . This result will give clear data of winglet performance at various angles of attack.

REFERENCES

[1]. Altab Hossain .G, AtaurRahman, A.K.M. Iqbal. P, Ariffin.M, and Mazian.M et.al, "Drag Analysis of an Aircraft Wing Model with and without Bird Feather like Winglet", World Academy of Science, Engineering and Technology International Journal of Mechanical, Industrial Science and Engineering Vol:5 No:9, 2011 .

[2]. Allen J.B, "Articulating Winglets",United States Patent Document,Patent No. US005988563, 1999

[3]. Ames.R, Smith.M.J, Komerath.N, Wong.O, "Performance Analysis of a Wing with Multiple Winglets",School of Aerospace Engineering, Georgia Institute of Technology, Atlanta, Georgia and J.Pearson, 2001, pp.2-3.

[4]. Azlin.M.Z, Mat Taib.C.F, Kasolang.S and Muhammad.F.H, "CFD Analysis of Winglets at Low Subsonic Flow",World Congress on Engineering 2011 Vol:1, 2011, pp. 1-5.

[5]. Bourdin.P,* Gatto.A,* and Friswell. M. I., "Aircraft Control via Variable Cant-Angle Winglets"Journal of Aircraft,Vol. 45, No. 2, March-April 2008. DOI: 10.2514/1.27720.pp. 414-423.

[6]. Bourdin.P,* Gatto.A,* and Friswell. M. I., "The Application of Variable Cant Angle Winglets for Morphing Aircraft Control", AIAA Journal – 24th Applied Aerodynamic Conference, 2006, pp. 1- 13.